Mol Neurobiol (2018) 55:4437–4452
DOI 10.1007/s12035-017-0669-1

Neuroprotective Effects of the Absence of JNK1 or JNK3 Isoforms on Kainic Acid-Induced Temporal Lobe Epilepsy-Like Symptoms

Luisa de Lemos[1,2] · Felix Junyent[1] · Antoni Camins[1,3,4] · Rubén Darío Castro-Torres[1,5] · Jaume Folch[3,6] · Jordi Olloquequi[7] · Carlos Beas-Zarate[5] · Ester Verdaguer[3,4,8] · Carme Auladell[3,4,8]

Received: 7 April 2017 / Accepted: 20 June 2017 / Published online: 29 June 2017

Abstract The activation of c-Jun-N-terminal kinases (JNK) pathway has been largely associated with the pathogenesis and the neuronal death that occur in neurodegenerative diseases. Altogether, this justifies why JNKs have become a focus of screens for new therapeutic strategies. The aim of the present study was to identify the role of the different JNK isoforms (JNK1, JNK2, and JNK3) in apoptosis and inflammation after induction of brain damage. To address this aim, we induced excitotoxicity in wild-type and JNK knockout mice (*jnk1*$^{-/-}$, *jnk2*$^{-/-}$, and *jnk3*$^{-/-}$) via an intraperitoneal injection of kainic acid, an agonist of glutamic-kainate-receptors, that induce status epilepticus.

Each group of animals was divided into two treatments: a single intraperitoneal dose of saline solution, used as a control, and a single intraperitoneal dose (30 mg/kg) of kainic acid. Our results reported a significant decrease in neuronal degeneration in the hippocampus of *jnk1*$^{-/-}$ and *jnk3*$^{-/-}$ mice after kainic acid treatment, together with reduced or unaltered expression of several apoptotic genes compared to WT treated mice. In addition, both *jnk1*$^{-/-}$ and *jnk3*$^{-/-}$ mice exhibited a reduction in glial reactivity, as shown by the lower expression of inflammatory genes and a reduction of JNK phosphorylation. In addition, in *jnk3*$^{-/-}$ mice, the c-Jun phosphorylation was also diminished.

Collectively, these findings provide compelling evidence that the absence of JNK1 or JNK3 isoforms confers neuroprotection against neuronal damage induced by KA and evidence, for the first time, the implication of JNK1 in excitotoxicity.

Luisa de Lemos and Felix Junyent contributed equally to this report.

Ester Verdaguer and Carme Auladell contributed as senior authors.

Electronic supplementary material The online version of this article (doi:10.1007/s12035-017-0669-1) contains supplementary material, which is available to authorized users.

✉ Carme Auladell
cauladell@ub.edu

[1] Unitat de Farmacologia i Farmacognòsia, Facultat de Farmàcia, Universitat de Barcelona, Avda Diagonal 641, E-08028 Barcelona, Spain

[2] Instituto Gulbenkian de Ciência, Rua da Quinta Grande 6, 2780-156 Oeiras, Portugal

[3] Networking Research Center on Neurodegenerative Diseases (CIBERNED), Instituto de Salud Carlos III, Madrid, Spain

[4] Neuroscience Institute, University of Barcelona, Barcelona, Spain

[5] Laboratorio de Regeneración Neural, Departamento de Biología Celular y Molecular, CUCBA, Universidad de Guadalajara, Guadalajara, Mexico

[6] Unitat de Bioquímica, Facultat de Medicina i Ciències de la Salut, Universitat Rovira i Virgili, Reus, Tarragona, Spain

[7] Facultad de Ciencias de la Salud, Instituto de Ciencias Biomédicas, Universidad Autónoma de Chile, Talca, Chile

[8] Departament de Biologia Cel·lular, Fisiologia i Immunologia, Facultat de Biologia, Universitat de Barcelona, Barcelona, Spain

Accordingly, JNK1 and/or JNK3 are promising targets for the prevention of cell death and inflammation during epileptogenesis.

Keywords c-Jun N-terminal kinase · Excitotoxicity · Hippocampus · Inflammation · Kainic acid · Knockout mice · Neurodegeneration · Neuroprotection

Introduction

The c-Jun N-terminal kinases (JNKs), a subfamily of MAP kinases (MAPK), are considered to be central signal transducers in the mammalian brain, mostly implicated in mediating the apoptotic response of cells induced by pro-inflammatory cytokines and genotoxic environmental stresses. However, JNK activation is also associated with the regulation of cell proliferation, cell survival, and cell differentiation [1]. Moreover, JNK regulates neurite formation and morphogenesis [2]. These antagonist functions can be explained by the signal intensity and duration; thus, transient JNK activation promotes cell survival, whereas prolonged JNK activation induces cellular apoptosis [3]. The involvement of the JNK pathway in these cellular processes reveals the importance of knowing how it acts in physiological and pathological conditions.

The JNK protein is activated by specific JNK kinases (JNKKs, MKK4, and MKK7) through dual phosphorylation on threonine and tyrosine residues. Once activated, JNK can translocate to the nucleus and control the expression of several transcriptional factors, such as c-Jun, ATF-2, and Elk-1 [4, 5]. In addition, JNK may also activate cytosolic substrates, such as those involved in cytoskeletal regulation [6, 7]. Other identified substrates have been the insulin receptor (IRS) [8], the functionally uncharacterized protein smoothelin-like 2 (SMTNL2) [9], or raptor protein, a key regulator of mTOR complex [10].

Considering that the JNK family consists of at least ten isoforms derived from the alternative splicing of three related genes, *jnk1*, *jnk2*, and *jnk3* [4], distinct substrate affinity is correlated with biological function. However, the specific function of each isoform is still unknown. The use of knockout mice for these isoforms has generated new data about their roles. Along this line, mice that lack individual isoforms of the JNK family are reported to be viable and survive with no phenotypic changes [11–13]. JNK3 has been largely associated with neuronal death and oxidative stress; this evidence is supported by different findings in *jnk3-null* mice that show a reduction of c-Jun phosphorylation in ischemia–hypoxia (Kuan et al. 2003), a decrease of cyt-c (cytochrome) release after spinal cord injury, and a significant increase in oligodendrocyte survival following traumatic injuries in the CNS [14, 15]. Furthermore, targeted disruption of the *jnk3* gene (but not *jnk1* or *jnk2)* rendered mice highly resistant to glutamate excitotoxicity, which was associated with a marked reduction in c-Jun phosphorylation and decreased activity of the AP-1 transcription factor complex [13, 16]. In addition, JNK3 and JNK2 are the main JNK isoforms that are implicated in stress-induced dopaminergic cell death in mice that is treated with MPTP (1-methyl-4-phenyl-1,2,4,6-tetrahydropyridine), a neurotoxin that replicates most of the neuropathological hallmarks of Parkinson's disease (PD) in humans [17]. Moreover, the genetic deletion of *jnk3* in familial Alzheimer's disease (AD) mice decreases β-amyloid plaque load, a hallmark of AD [18]. On the other hand, JNK1 and JNK2 have been associated with developmental brain processes; the $jnk1^{-/-}jnk2^{-/-}$ compound mutation leads to neural tube defects and embryonic lethality [19]. Moreover, the JNK1 and JNK2 isoforms participate in apoptosis regulation during normal brain development [20]. JNK1-deficient mice exhibit progressive degeneration of long nerve fibers and a loss of microtubule integrity, associated with hypophosphorylation of MAP2 (microtubule-associate proteins) and other MAP proteins [6, 7]. These studies demonstrate the role of c-Jun N-terminal kinases in the progression of brain damage and cell integrity with differential isoform specificity. In particular, JNK3 is mainly involved in neuronal death; whereas, JNK1 has a pivotal role in processes that are closely related to cell plasticity. In addition, different studies evidenced that JNK1 plays a major role in the development of obesity and insulin resistance [8].

In this study, we proposed to examine the role of the different JNK isoforms specifically in neuronal death and in inflammation processes. To address this aim, we induced excitotoxicity in wild-type (WT) and JNK knockout (KO) mice ($jnk1^{-/-}$, $jnk2^{-/-}$, *and* $jnk3^{-/-}$) via an intraperitoneal (i.p.) injection of kainic acid (KA), a potent neurotoxic agent that is an agonist of α-amino-3-hydroxy-5-methyl-4-isoxazolepropionic acid (AMPA)/kainate receptors. This neurotoxin is able to induce severe status epilepticus (SE), characterized by recurrent motor seizures and neuronal damage in the limbic system, particularly in the hippocampus, accompanied by reactive gliosis. The KA experimental model was originally discovered by Ben-Ari [21, 22] and has been extensively used over the past decades because of their high level of similarity with human epilepsy [23–25]. JNK pathway has been shown to play a key role in the process of neuronal death induced with KA [26–29]. In this way, our results showed that disruption of *jnk1* or *jnk3* genes reduces the occurrence of seizures after KA injections and prevents neuronal damage. Furthermore, most of the apoptotic genes that were analyzed were less induced or unaltered in $jnk1^{-/-}$ and $jnk3^{-/-}$ mice relative to WT treated mice. Moreover, in $jnk1^{-/-}$ and $jnk3^{-/-}$ mice, we observed a reduction in glial reactivity, based on the decreased expression of inflammatory genes, together with lower levels of phospho-JNK (pJNK) and phospho c-Jun

(p-c-Jun). Altogether, these findings provide evidence that the absence of JNK1 or JNK3 isoforms confers neuroprotection against the neuronal damage induced by KA, highlighting, for the first time, the role of JNK1 in brain harm following excitability. Moreover, the data revealed that the neuroprotection induced with the lack of JNK1 or JNK3 occurs through different pathways. Consequently, our results emphasize JNK1 and/or JNK3 as promising targets for the prevention of cell death and inflammation during epileptogenesis.

Experimental Procedure

Animal Husbandry

Two-month-old C57BL/6 WT and knockout mice were used for JNK (*jnk1*$^{-/-}$, *jnk2*$^{-/-}$, *jnk3*$^{-/-}$) in this study. The generation and characterization of *jnk1*$^{-/-}$ [11], *jnk2*$^{-/-}$ [12], and *jnk3*$^{-/-}$ [13] single knockout mice have been previously described. The mice were backcrossed to C57BL/6 mice. Throughout the experiments, all mice were housed individually in a controlled environment. Food and water were available ad libitum. The experiments were conducted in accordance with the Council of Europe Directive 2010/63. The procedure was registered at the *Department d'Agricultura, Ramaderia i Pesca* of the *Generalitat de Catalunya*. Ref. Number order 8852.

Kainic Acid Treatment and Sample Preparation

Four groups of 2-month-old mice were established (WT, *jnk1*$^{-/-}$, *jnk2*$^{-/-}$, and *jnk3*$^{-/-}$). Each group was divided into two conditions: mice treated with a single i.p. dose of saline solution, used as a control, and mice treated with a single i.p. dose (30 mg/kg) of KA (Sigma-Aldrich, USA) [30, 31].

Following injection, animals were returned to cages where seizures appeared after 10 min and lasted for 2 h. The animals used for the study were the ones that presented stage 5 (continuous rearing and falling) or 6 (severe whole-body convulsions) of the Racine scale [30, 32]. The sacrifice of the animals was done after KA injection at different times which vary depending on the method used, 12 h for RNA analysis, 24 h for Fluoro-Jade B stain, 24 h and 3 d for immunochemistry and immunofluorescence, and for western blot analyses at 3 and 6 h. Mice were anesthetized by i.p. injection of 80 mg/kg pentobarbital.

Fluoro-Jade B Staining

Neurodegeneration was assessed using Fluoro-Jade B (FJ) (Chemicon Europe Ltd.). Slides with brain tissue samples that were obtained from WT, *jnk1*$^{-/-}$, *jnk2*$^{-/-}$, and *jnk3* mice were rinsed with phosphate-buffered saline (PBS), followed by two washes in distilled water. Afterwards, slides were immersed in 0.6 g/L of potassium permanganate (KMnO4) for 15 min in the dark. Then, after two washes in distilled water, the slides were transferred to a staining solution that contained 0.1 mL/L acetic acid and 0.004 mL/L FJ for 30 min in the dark. Cell nuclei were stained with Hoechst 33342 50 nM (Sigma-Aldrich, USA). Slides were rinsed in distilled water, dried, and then submerged directly into xylene and mounted with DPX medium. The samples were analyzed with an epifluorescence microscope (Olympus BX61, Olympus IBERIA S.A.U, Spain). FJ^{+} cells in the CA3 region were evaluated. Sections that corresponded to the hippocampal levels between Bregma −1.28 to −2.12 mm, in accordance with the Paxinos and Franklin atlas (2012), were used to calculate the number of FJ^{+} cells in the CA3 area of each section (four to six animals per genotype, four to eight sections per animal).

RNA Extraction and Quantitative Real-time PCR

Animals were decapitated 12 h after the KA injection and the brain was quickly removed. The hippocampi from WT, *jnk1*$^{-/-}$, *jnk2*$^{-/-}$, and *jnk3*$^{-/-}$ mice were rapidly dissected, immediately frozen on dry ice, and stored at −80 °C until use.

Total RNA was isolated from the hippocampi using Trizol (Invitrogen, Carlsbad, CA, USA) followed by chloroform treatment according to the manufacturer's protocol. RNA concentration was measured with a NanoDropTM 1000 Spectrophotometer (Thermo Scientific, MA, USA).

As a general procedure, 1 μg of total RNA was reverse transcribed using a high-capacity complementary DNA (cDNA) reverse transcription kit (Applied Biosystems, Carlsbad, CA, USA). The same amounts of cDNA were subsequently used for quantitative real-time PCR with SYBR Green® PCR Master Mix and PCR was performed on the StepOnePlus™ Real-time PCR system (Applied Biosystems, Carlsbad, CA, USA). All samples were run in triplicate, and expression values were normalized to the *housekeeping gene β-actin* in the same reaction. Relative normalized messenger RNA (mRNA) levels were calculated using the $2^{-\Delta\Delta Ct}$ method. Gene-specific primers corresponding to the PCR targets on the PCR RT2 array were designed using Primer Express® Software v2.0 (Applied Biosystems, Carlsbad, CA, USA). The following primer sequences were used for quantitative real-time PCR experiments: *Atf5*: forward 5′GGGTCATT TTAGCTCTGTGAGAGAA3′ and reverse 5′ATTTGTGC CCATAACCCCTAGA3′; *Bcl10* forward 5′GGCCTGGA CACCCTGGTGGAA3′ and reverse 5′GCTGCTGC ATTCAGGCCTTTG3′; *Casp3* forward 5′TCAGAGGC GACTACTGCCGGA3′ and reverse 5′GTACCCGG CAGGCCTGAAT3′; *Casp4* forward 5′ACGCAGTG ACAAGCGTTGGGTTT3′ and reverse 5′TGGTGCCT GGGTCCACACTG3′; *Casp8* forward 5′GGCACCAG

GATGCCACCTCT-3′ and reverse 5′CTGTTCCACGCGCT CACA3′; *Ccl2* forward 5′CCCACTCACCTGCTGCTACT3′ and reverse 5′TCTGGACCCATTCCTTCTTG3′; *Cidea* forward 5′GGACTACGCGGGAGCCCTCA3′ and reverse 5′ ATCACCCCACGCCGGCTACT3′; *Cox2* forward 5′ TGACCCCCAAGGCTCAAATA3′ and reverse 5′ CCCAGGTCCTCGCTTATGATC3′; *Fas* forward 5′ GTAACCAACCTGCGCCCCA3′ and reverse 5′ CACACGAGGCGCACGAACA-3′; *Fasl* forward 5′ TGGTGGCTCTGGTTGGAATGGGA3′ and reverse 5′ AGGCTTTGGTTGGTGAACTCACG3′; *Ifnγ* forward 5′ CGGCACAGTCATTGAAAGCC3′ and reverse 5′ TGTCACCATCCTTTTGCCAGT3′; *Il1β* forward 5′ ACAGATATCAACCAACAAGTGATATTCTC3′ and reverse 5′GATTCTTTCCTTTGAGGCCCA3′; *Mcl1* forward 5′CGAGACGGCCTTCCAGGGCAT3′ and 5′TCCTGCCC CAGTTTGTTACGCC3′; *Pak7* forward 5′ACCCCAGA GGCCCCACCAAA3′ and reverse 5′AGGGTACT GGTGGCTGCCTGA3′, *Tnfα1* forward 5′TCGGGTGA TGGTCCCCAA3′ and reverse 5′TGGTTTGCTACGAC GTGGGCT3′; *Tnfr1* forward 5′GTGCGCCCTTGCAG CCAT3′ and reverse 5′GCAACAGCACCGCAGTACCT GA3′; *Traf2* forward 5′GCCTGACCAGCATCCTCAGC TCT3′ and reverse 5′ACCTCTCTGCGGGCAGCGTTA3′; *β-actin* forward 5′CAACGAGCGGTTCCGAT3′ and reverse 5′GCCACAGGATTCATACCCA3′.

Immunofluorescence

Immunofluorescence experiments were conducted with the different groups of mice (WT, *jnk1*$^{-/-}$, *jnk2*$^{-/-}$, and *jnk3*$^{-/-}$) treated with saline solution and used as controls, and the same groups were treated with KA and sacrificed 24 h and 3 d after injection. Animals were perfused with 40 g/L of paraformaldehyde in 0.1 mol/L of phosphate buffer, and the brains were removed. The brains were subsequently rinsed in the same solution with 300 g/L of sucrose for 24 h and then frozen. Coronal sections of 20 μm were obtained with a cryostat (Leica Microsystems, Wetzlar, Germany).

Free-floating coronal sections, 20 μm thick, were rinsed in 0.1 mol/L phosphate buffer (PB), pH 7.2. After that, sections were pre-incubated in a blocking solution (100 mL/L of fetal bovine serum (FBS), 2.5 g/L of bovine serum albumin, and 0.2 mol/L of glycine in PBS with 5 mL/L Triton X-100) at room temperature (RT). Then, the samples were incubated overnight (O/N) at 4 °C with different primary antibodies: rabbit anti-GFAP (1:2000; DAKO, Glostrop, Denmark), rabbit anti-Iba1 (1:1000; WAKO, Osaka, Japan), and rabbit anti-p-c-Jun (1:700; Cell Signaling). Sequentially, the sections were incubated for 2 h with Alexa Fluor 594 goat anti-rabbit antibody (1:500; Invitrogen, Eugene, OR, USA) and counterstained with 0.1 μg/mL Hoescht 33258 (Sigma-Aldrich, USA) nuclear stains for 5 min in the dark. Immediately after that, the samples were rinsed with PBS and were mounted onto gelatinized slides with Fluoromount medium (Sigma-Aldrich, USA). The stained sections were examined under an epifluorescence microscope (Olympus BX61).

Quantification of Immunofluorescence of GFAP and Iba1

The Iba1 and GFAP cells were evaluated in the CA1 region. Area fraction was calculated as previously described by [33]. Briefly, the CA1 hippocampal area was identified and photographed at ×20. Then, the images captured were transformed to 8-bit gray scale and normalized, highlighting the area occupied by the fluorescent signal of Iba1 and GFAP cells under fixed threshold using the NIH ImageJ software. The sections used correspond to the hippocampal levels between Bregma −1.28 to −2.12 mm, in accordance with the Paxinos and Franklin atlas (2012) [34] (four to six animals per genotype, four to eight sections per animal).

Western Blot

The animals were treated with KA and sacrificed at different time points (3 and 6 h). The hippocampi from the different animals were homogenized with lysis buffer (137 mM NaCl, 20 mM Tris-HCl, pH 8.0, 1% NP 40, 10% glycerol, 1 mM PMSF, 10 μg/mL aprotinin, 1 μg/mL leupeptin, and 0.5 mM sodium orthovanadate). Homogenates were spun at 13,000 rpm for 20 min at 4 °C, and the protein content of the supernatants was determined with the BCA method (Pierce Company, Rockford, MI, USA). A total of 10 μg of protein was mixed 1:1 (*v*:*v*) with a loading buffer (β-mercaptoethanol 100 mM, Tris-HCl pH 6.8, 2% sodium dodecyl sulfate, SDS) and denatured at 95 °C for 5 min. Samples were loaded in 12% SDS-PAGE (sodium dodecyl sulfate polyacrylamide gel electrophoresis) at 90 V for 2–3 h and transferred overnight at 4 °C and 35 V to a PVDF membrane (0.45 μm, Millipore, Bedford, MA, USA). The membrane was blocked in 10% non-fat milk in TBS-Tween, pH 7.4, for 4 h at RT. Afterwards, the membrane was incubated with specific primary antibodies for JNK1, JNK2, JNK3, p-JNK, total JNK, p-c-Jun and total c-Jun (1:1000, Cell Signaling Technology, USA), and β-actin (1:20,000, Sigma-Aldrich, USA) O/N at 4 °C. After several washes, the membrane was further incubated with a secondary antibody diluted at 1:2000 in TBS-Tween for 1 h at RT. The signals were developed with chemiluminescent substrate (ECL™ Western Blotting Analysis System, GE Healthcare, UK) before film exposure (Medical X-ray film, Fujifilm Spain). β-Actin was used to normalize differences in gel loading. Semi-quantitative values were obtained using the Image Lab software (Bio-Rad, USA).

Data Processing and Statistical Analysis

Student's *t* test was performed to compare two conditions and a one-way ANOVA followed by a Bonferroni post hoc test was used to compare three or more conditions. Differences were considered significant at $P < 0.05$ (*, #), $P < 0.01$ (**, ##), and $P < 0.001$ (***, ###). Differences in gene expression between samples were evaluated using independent samples *t* tests.

Results

Cell Death Reduction in the Hippocampal Areas of *jnk3*$^{-/-}$ and *jnk1*$^{-/-}$ Mice Treated with KA

FJ is a fluorochrome that is commonly used to label degenerating neurons [35]. Our results demonstrated a higher number of FJ$^+$ cells after 24 h of KA treatment, mainly in the CA3 area of the hippocampus; FJ$^+$ cells may also be present in other areas such as the cortical regions, the thalamus and the amygdala (data not shown). However, no FJ$^+$ cells were observed in the control animals. Interestingly, a reduction in the number of FJ$^+$ cells was found in *jnk1*$^{-/-}$ and *jnk3*$^{-/-}$ treated mice compared to WT and *jnk2*$^{-/-}$ treated mice (Fig. 1).

Inflammatory Response After KA Treatment in WT and JNK Knockout Mice

jnk1$^{-/-}$ *and jnk3*$^{-/-}$ *Mice Exhibit a Reduced Reactive Astrocyte Response After KA Treatment*

To determine the effects of JNK isoforms on the inflammatory response, we evaluated in the hippocampus of WT, *jnk1*$^{-/-}$, *jnk2*$^{-/-}$, and *jnk3*$^{-/-}$ mice, 24 h and 3 d after KA treatment, the microglial response and astroglial activation, considered markers of neurotoxicity [36]. To do this, immunofluorescences were performed for Iba1, a protein upregulated in the activated microglia, and for GFAP, the intermediate filament system of adult astrocytes which is used as an astrogliosis

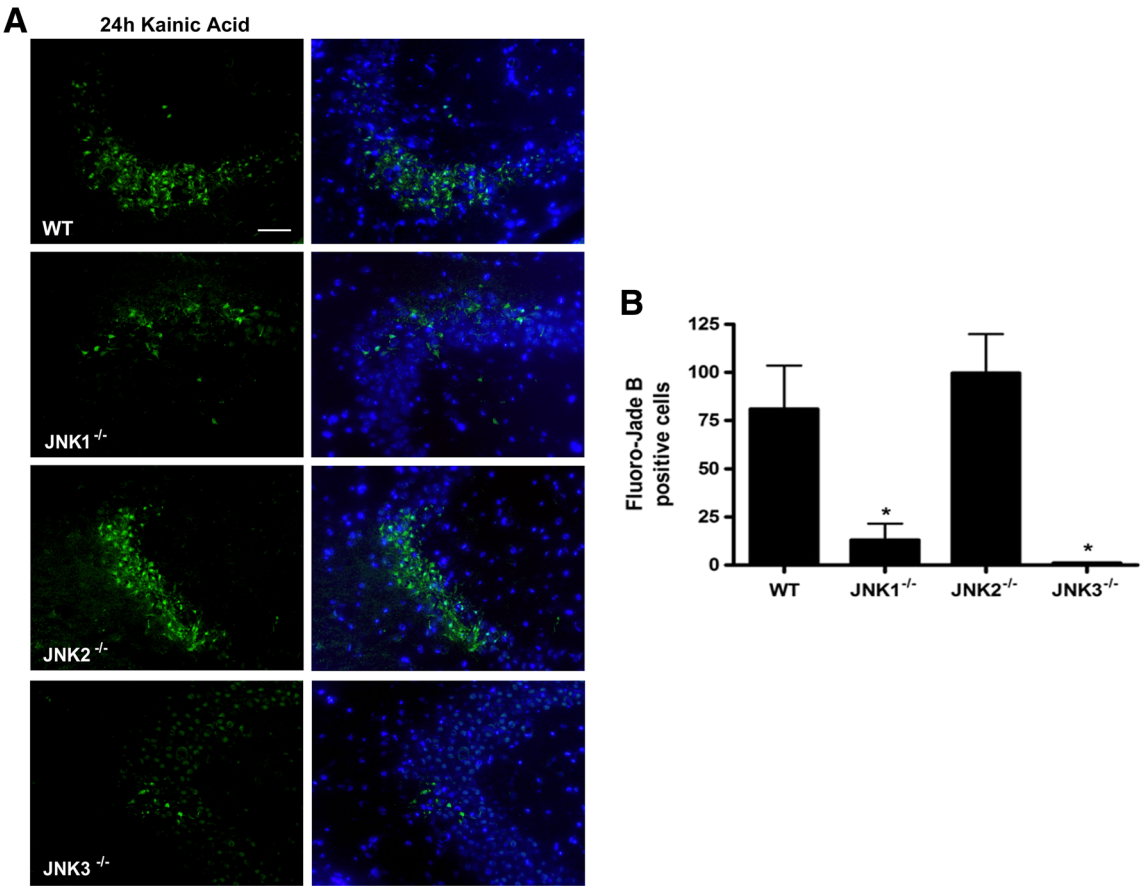

Fig. 1 Fluoro-Jade B labeling in the CA3 hippocampal area of WT, *jnk1*$^{-/-}$, *jnk2*$^{-/-}$, and *jnk3*$^{-/-}$ mice following 24 h of KA administration. The positive cells to Fluoro-Jade B are seen on the *green fluorescence* and in the nuclei stained by Hoeschst on the *blue fluorescent*. **a** A reduction in the number of FJ$^+$ neurons is observed in *jnk3*$^{-/-}$ and *jnk1*$^{-/-}$ mice compared to that in WT and *jnk2*$^{-/-}$ mice. *Scale bar* 50 μm. **b** The graph shows the quantification of FJ$^+$ neurons in CA3 area of the hippocampus of WT, *jnk1*$^{-/-}$, *jnk2*$^{-/-}$, and *jnk3*$^{-/-}$ mice at 24 h after KA administration. Each point is the mean ± SEM of three independent experiments (*$P < 0.05$)

marker. The results revealed less Iba1 and GFAP immunoreactivity in *jnk3*$^{-/-}$ mice than that in the other genotypes (Figs. 2a and 3a). In addition, we surprisingly observed that the lack of JNK1 was related to a reduction in astrogliosis, 3 d after KA treatment (Fig. 3). The evaluation of immunostain supported these results (Figs. 2b and 3b).

jnk1$^{-/-}$ *and jnk3*$^{-/-}$ *Mice Exhibit Reduced Expression Levels of Pro-Inflammatory-Related Genes After KA Treatment*

To better understand the differential microglial response observed in *jnk1*$^{-/-}$ and *jnk3*$^{-/-}$ KA treated mice, we evaluated the expression levels of several genes involved in the inflammatory response via real-time PCR. We analyzed the mRNA levels of *Interleukin-1β* (*il1β*) gene, one of the major mediators of the immune response that has an important role in the induction of neurodegeneration; *interferon gamma* (*ifnγ*) gene, a positive factor that promotes the inflammatory reaction; *monocyte chemoatractant protein-1* (*mcp-1/ccl2*) gene, a small cytokine that recruits cells of the immune system to the sites of inflammation and *cyclooxygenase 2* (*cox2*) gene, responsible for formation of prostanoids, mediators of inflammatory reactions. The mRNA levels of *ifnγ* increased after KA treatment in the different genotypes, except in *jnk3*$^{-/-}$ mice, in which the levels were unchanged. The expression level of *il1β* were also different in *jnk3*$^{-/-}$ mice compared to the other genotypes, as it is seen in figure 4a, where *il1β* mRNA levels were undetectable. The mRNA levels of *mcp-1/ccl2* and *cox2* increased in all genotypes after KA treatment; however, the levels in *jnk1*$^{-/-}$ and *jnk3*$^{-/-}$ mice were significantly lower compared to those in WT and *jnk2*$^{-/-}$ treated mice (Fig. 4).

Differential Responses in Apoptotic-Related Genes between JNK Knockout Mice and WT Mice Following KA Injection

In a previous study, 84 genes related to apoptosis were analyzed using a real-time PCR array (Mouse Apoptosis RT2 Profiler PCR Array) in order to assess whether apoptosis-related genes showed expression changes in mice. The results indicated that the administration of KA caused significant expression changes in 23 genes [37]. The analyses did at different times (3, 6, 12, and 24 h) after KA injection, revealing that 12 h was the optimum time to detect clear differences in gene expression between treated genotypes (data not shown). Accordingly, in our present work, the expression levels of these genes were analyzed in KO mice after 12 h of KA treatment. Thus, the expression levels of *tnfα*, *tnfr1*, and *fasr* genes, all of which are related to the extrinsic apoptotic pathway, were upregulated in all of the groups of mice, except, the expression levels of *fasl* that were maintained in *jnk1*$^{-/-}$ and *jnk3*$^{-/-}$ relative to those in untreated mice (Figs. 5 and 9). On the other hand, the expressions of caspase genes (*casp3*, *casp4*, and *casp8*), which play essential roles in programmed cell death, were upregulated after KA treatment in WT and *jnk2*$^{-/-}$ mice while in *jnk1*$^{-/-}$ and *jnk3*$^{-/-}$ mice, the expression levels were maintained (Fig. 6). In addition, in *jnk3*$^{-/-}$ mice, differential expression levels of some apoptotic genes were observed compared to the other genotypes after KA treatment. Specifically, *bcl10* and *mcl1* were upregulated, and *cradd* was downregulated in WT, *jnk1*$^{-/-}$, *and jnk2*$^{-/-}$ mice, while in *jnk3*$^{-/-}$ mice, the levels of these genes were maintained relative to that in the untreated mice (Figs. 7 and 9). Furthermore, the pro-apoptotic gene *cidea* had a genotype-dependent differential response: whereas KA treatment induced a downregulation of *cidea* in WT and *jnk2*$^{-/-}$ mice, an upregulation was detected in *jnk3*$^{-/-}$ mice. In the case of *jnk1*$^{-/-}$ mice, no significant changes were observed (Figs. 7 and 9). Otherwise, the expression of *atf5*, *traf2*, and *pak7* genes, which mainly mediate crucial anti-apoptotic signals, was unchanged in *jnk1*$^{-/-}$ and *jnk3*$^{-/-}$ mice (Figs. 8 and 9).

JNK Pathway Activation After KA Treatment

Reduction of JNK Phosphorylation After KA Treatment in jnk1$^{-/-}$ *and jnk3*$^{-/-}$ *Mice*

JNK plays an essential role in the stimulation of apoptotic signaling through its ability to interact and modulate the activities of diverse pro- and anti-apoptotic proteins. The results reported here revealed differences between the different JNK isoforms in the basal activation of pro-apoptotic JNK (p-JNK/JNK ratio) in the mouse hippocampus. Thus, western blot analyses revealed a marked decrease in the p-JNK/JNK ratio in *jnk1*$^{-/-}$ and *jnk3*$^{-/-}$ at 3 and 6 h after KA treatment related to that in the WT mice (Fig. 10), which suggests a role of JNK1 and JNK3 isoforms in the induction of apoptosis.

Reduction of c-Jun Phosphorylation After KA Treatment in jnk3$^{-/-}$ *Mice But Not in jnk1*$^{-/-}$ *Mice*

Increased expression of the *c-jun* and high levels of c-Jun phosphorylation precede or coincide with periods of cell death and occur following seizures [38]. The results obtained with western blot and immunofluorescence revealed high levels of p-c-Jun in WT mice after KA treatment, as expected (Figs. 11 and 12). By western blot, a reduction in p-c-Jun levels was observed in *jnk3*$^{-/-}$ mice compared with that in WT, after 3 and

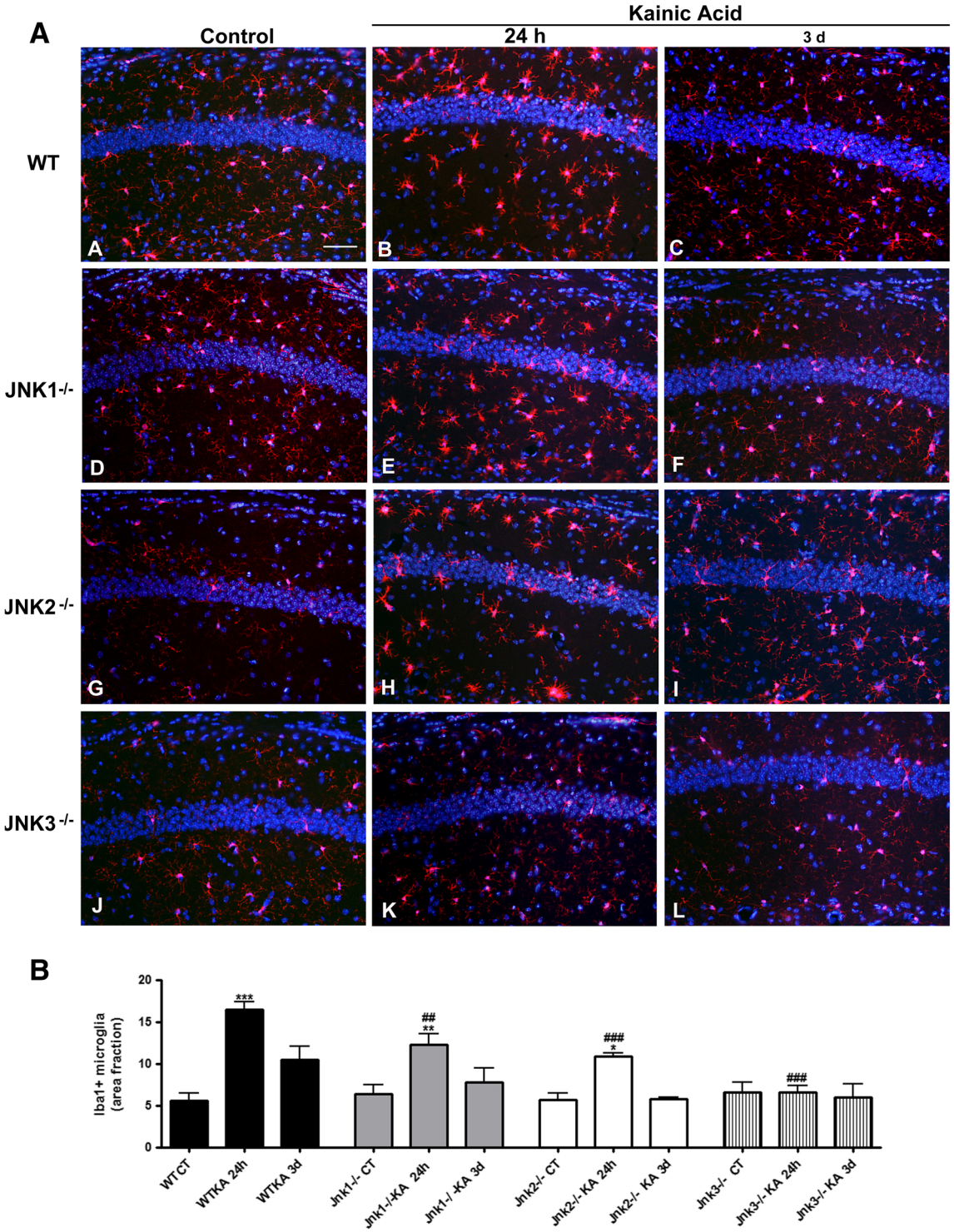

Fig. 2 Immunofluorescence against Iba-1 (*red*) at 24 h and 3 days after KA treatment in the CA1 hippocampal area. WT (*A–C*), *jnk1*$^{-/-}$ (*D–F*), *jnk2*$^{-/-}$ (*G–I*), and *jnk3*$^{-/-}$ mice (*J–L*). *A* A reduction in the number of microglial cells was observed after 24 h of KA injection, in *jnk3*$^{-/-}$ mice (*K*) vs the other genotypes (*B*, *E*, and *H*). *Scale bar* 50 μm. *B* Quantification of Iba1 positive cells is shown in the bar graphs. Each point is the mean ± SEM of 3–6 independent experiments (*$P < 0.05$, **$P < 0.01$, ***$P < 0.001$ vs each CT isoform; $^{\#\#}P < 0.01$, $^{\#\#\#}P < 0.001$vs WT KA 24 h)

6 h of KA treatment. The diminution in *jnk1*$^{-/-}$ was observed after 6 h of KA treatment but not after 3 h. Thus, the pattern of p-c-Jun levels following KA treatment was similar in *jnk1*$^{-/-}$ and *jnk2*$^{-/-}$ mice (Fig. 11).

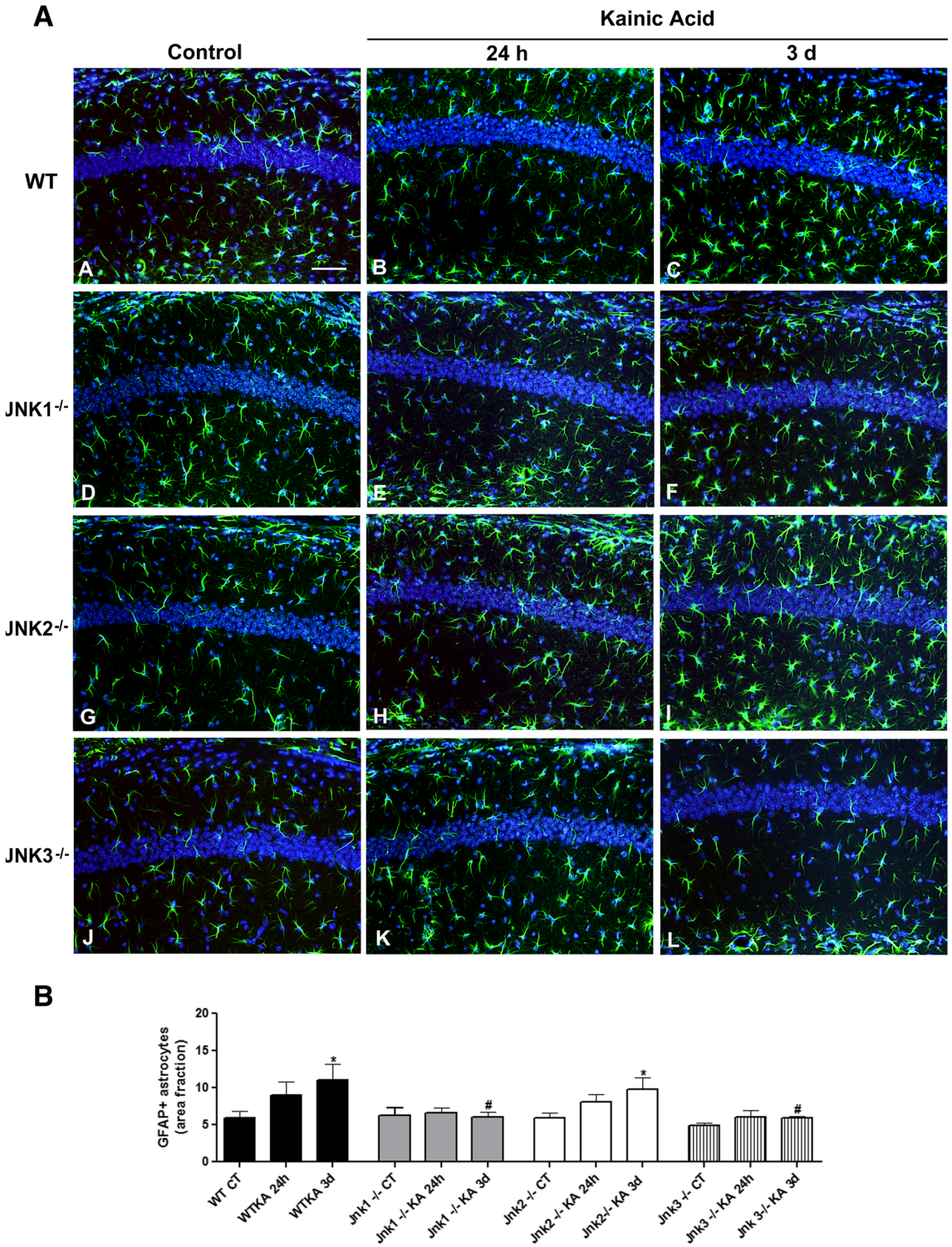

Fig. 3 *A* Immunofluorescence against GFAP (*green*) at 24 h and 3 days after KA treatment in the CA1 hippocampal area. WT (*A–C*), *jnk1*$^{-/-}$ (*D–F*), *jnk2*$^{-/-}$ (*G–I*), and *jnk3*$^{-/-}$ mice (*J–L*). A reduction in astrocyte cells was observed after 3 days of KA injection, in *jnk1*$^{-/-}$ and *jnk3*$^{-/-}$ mice (*F* and *L*) vs the increase observed in WT and *jnk2*$^{-/-}$ mice (*C* and *I*). *Scale bar* 50 μm. *B* Bar graphs represent the quantification of GFAP-positive cells of 3–6 independent experiments. Each point is the mean ± SEM. (*$P < 0.05$, vs each CT isoform; $^{\#}P < 0.05$ vs WT KA 3d)

The data obtained by immunofluorescence against p-c-Jun revealed a reduction of this protein in the CA3 area in both *jnk1*$^{-/-}$ and *jnk3*$^{-/-}$ mice, after 3, 6, and 12 h of KA treatment in contrast with what occurs in WT and *jnk2*$^{-/-}$ mice (Fig. 12).

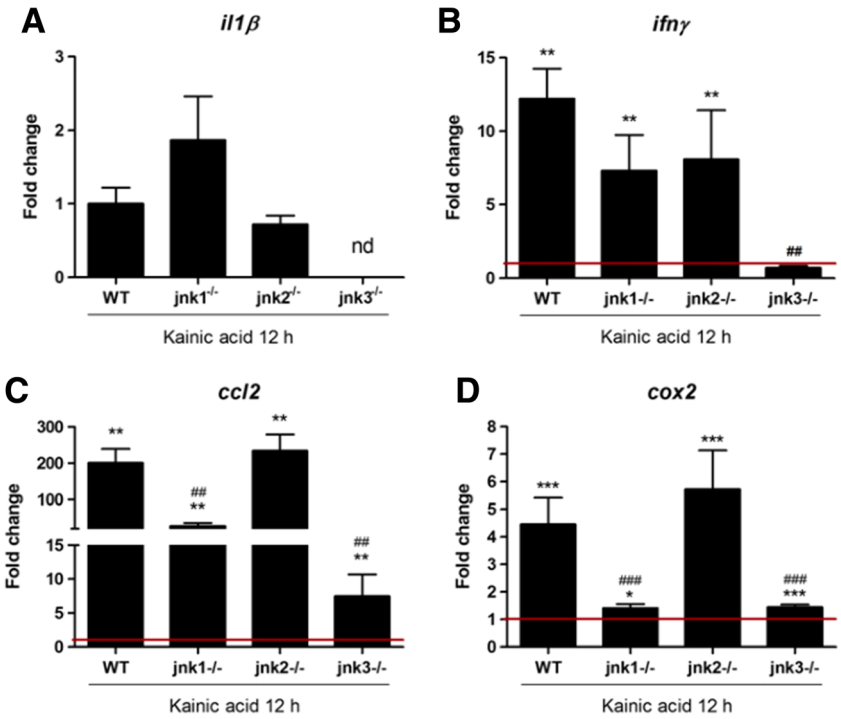

Fig. 4 Quantitative PCR (qPCR) analysis of **a** *il1β*, **b** *ifnγ*, **c** *ccl2*, and **d** *cox2* mRNA expression levels in the hippocampus of WT, *jnk1*$^{-/-}$, *jnk2*$^{-/-}$, and *jnk3*$^{-/-}$ mice after 12 h of KA treatment. The results are presented in terms of a fold change after normalizing to β-actin mRNA levels. Each value represents the mean ± SEM of six independent experiments. $^{**}P < 0.01$ and $^{***}P < 0.001$ vs basal control; $^{\#\#}P < 0.01$ and $^{\#\#\#}P < 0.001$ vs WT after 12 h of KA treatment (kainic acid 12 h)

Discussion

In the present study, we reported that the absence of JNK1 or JNK3 isoforms in mice reduces neurotoxicity after KA treatment. Whereas the lack of JNK3 has been widely related to neuroprotection in different diseases, such as epilepsy, Parkinson's disease, ischemia, and Alzheimer's disease ([13]; Kuan et al. 2003; [16, 18, 39]), JNK1 has mainly been linked with other cellular functions, such as neurogenesis and axonal and dendritic architecture control, despite being related to apoptosis. Interestingly, in this study, we report for the first time that the lack of JNK1 is able to protect against excitotoxicity, which occurs with the absence of JNK3, albeit through different cell mechanisms.

Reduction of Neuronal Damage in *Jnk1*$^{-/-}$ and *Jnk3*$^{-/-}$ Mice After KA Treatment

JNK is a multifunctional kinase involved in many physiological and pathological processes [40, 41]. The FJ stain revealed that the lack of JNK1 or JNK3 isoforms reduces neuronal damage in the brains treated with KA. This decrease was correlated to a diminution of JNK and c-Jun phosphorylation, since the WB and immunofluorescence analyses showed a reduction in p-c-Jun and p-JNK levels after KA treatment, compared to other genotypes. However, in *jnk1*$^{-/-}$ mice, although a reduction in the CA3 area of immunopositive p-c-Jun cells was detected, as occurred in *jnk3*$^{-/-}$ mice, by WB this diminution was not observed. These differences observed

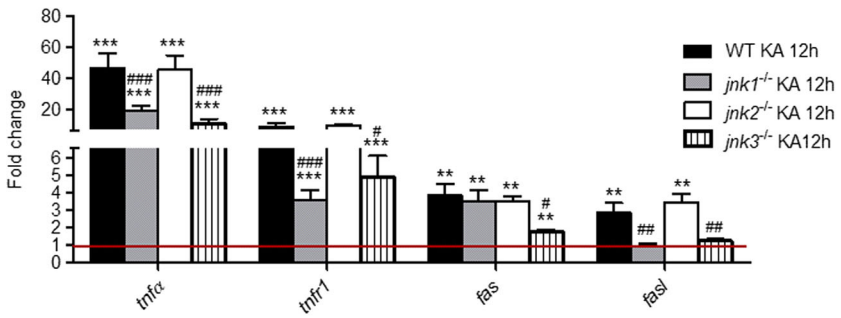

Fig. 5 Apoptotic extrinsic genes. Fold change detection of *tnfα*, *tnfr1*, *fas*, and *fasl* mRNA expression levels in WT, *jnk1*$^{-/-}$, *jnk2*$^{-/-}$, and *jnk3*$^{-/-}$ mice 12 h after KA treatment compared to those in untreated mice. Each value represents the mean ± SEM (n = 6/group). *Red baseline* indicates the basal expression level in untreated mice for each gene. $^{**}P < 0.01$ and $^{***}P < 0.001$ vs basal control; $^{\#}P < 0.05$, $^{\#\#}p < 0.01$, $^{\#\#\#}P < 0.001$ vs WT KA 12 h

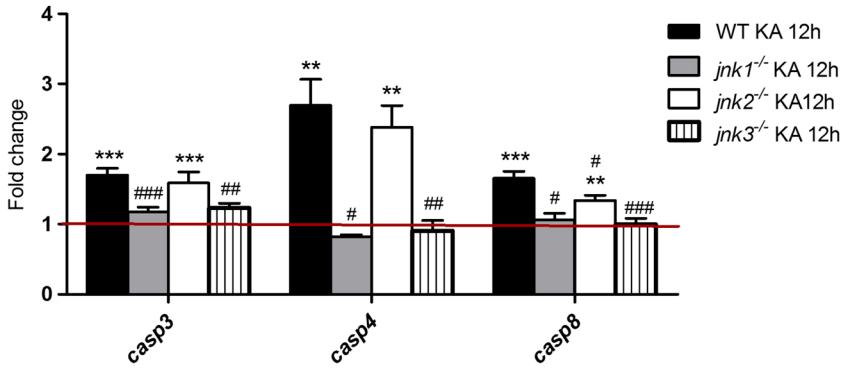

Fig. 6 Caspase genes. Fold change detection of c*asp3*, *casp4*, and *casp8* mRNA expression levels in WT, *jnk1*$^{-/-}$, *jnk2*$^{-/-}$, and *jnk3*$^{-/-}$ mice 12 h after KA treatment. Each value represents the mean ± SEM (n = 6/group). The *red baseline* indicates the basal expression level in untreated mice for each gene. $^{**}P < 0.01$ and $^{***}P < 0.001$ vs basal control WT; $^{\#}P < 0.05$, $^{\#\#}P < 0.01$, $^{\#\#\#}P < 0.001$ vs WT KA 12 h

between WB and immunofluorescence could be explained because by WB the whole hippocampus is analyzed, whereas by immunofluorescence a specific area and the localization of the protein are detected. Furthermore, these data point at that JNK1 and JNK3 have different targets in order to induce neural death. In this line, the results obtained by Park [42] evidenced that Smac/Diablo, a mitochondrial protein that promotes caspase activity, is a major physiological substrate of JNK1 in the regulation of apoptosis.

The reduction of neuronal damage was correlated with the higher survival of *jnk1*$^{-/-}$ and *jnk3*$^{-/-}$ mice in comparison to WT, after KA injection (data not shown). The relation between the absence of JNK3 and the reduction of neuronal death after brain excitotoxicity is in accordance with previous studies ([13, 16]; Kuan et al. 2003). However, JNK1 isoform, despite being related to apoptosis, has largely been linked with other cellular functions, such as neurogenesis and neuronal differentiation [29, 43], architecture dendritic regulation [44], axonal regeneration control [45], and insulin resistance [8]; therefore, to the best of our knowledge, this is the first time that the lack of JNK1 showed neuronal damage reduction after brain excitability.

All these results support that JNK1 and JNK3 have a key role in brain injury after KA treatment and that it takes place through distinct mechanisms.

JNK1 and JNK3 Isoforms Differentially Regulate Neuroinflammatory Mechanisms Induced After KA

Astrocytes and microglia are considered key players in the initiation of an inflammatory response after injury in the CNS [46]. Specifically, astrogliosis and microglial reactivity have been extensively described after KA injection [14, 15, 47]. Therefore, the reduction in reactive astrocytes found in *jnk1*$^{-/-}$ and *jnk3*$^{-/-}$ treated mice was relevant. These data again support the finding of neuroprotection against KA in the absence of JNK1 or JNK3 isoforms. Moreover, it was interesting that whereas astrogliosis was reduced in both KO mice, microglial reactivity was depleted only in *jnk3*$^{-/-}$ and not in *jnk1*$^{-/-}$ mice. These data evidenced that JNK1 and JNK3 interfere in the astrocyte response after brain damage induction and pointed out that JNK3 isoform participates on microglial response against KA. Probably, these actions would be related to a reduction in JNK activity; however,

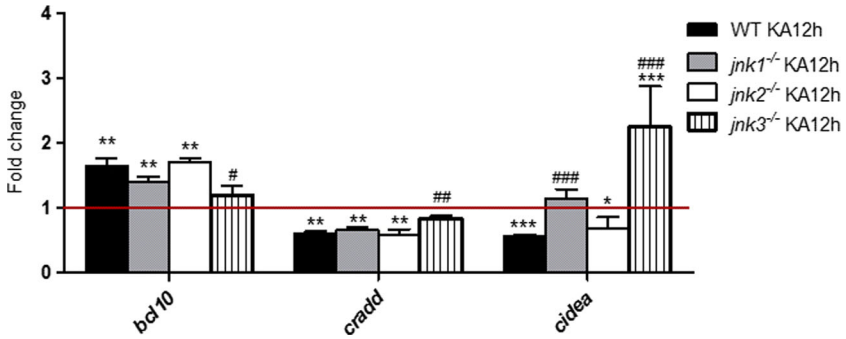

Fig. 7 Genes that regulate apoptosis. Fold change detection of *bcl10*, *cradd*, and *cidea* mRNA expression levels in WT, *jnk1*$^{-/-}$, *jnk2*$^{-/-}$, and *jnk3*$^{-/-}$ mice 12 h after KA treatment. Each value represents the mean ± SEM (n = 6/group). The *red baseline* indicates the basal expression level in untreated mice for each gene. $^{**}P < 0.01$ and $^{***}P < 0.001$ vs basal control WT; $^{\#}P < 0.05$, $^{\#\#}P < 0.01$, $^{\#\#\#}P < 0.001$ vs WT KA 12 h

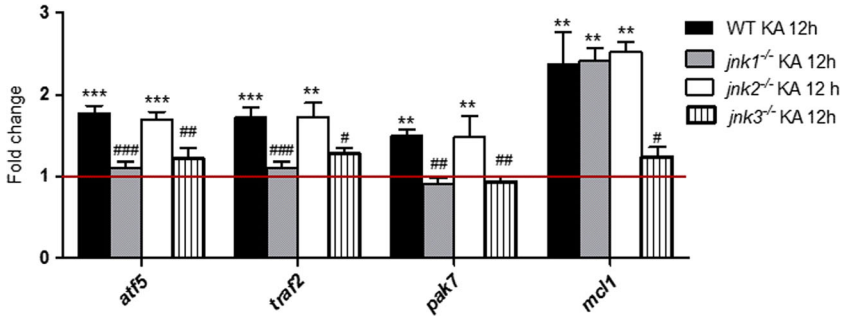

Fig. 8 Negative regulation of the apoptosis process. Fold change detection of *atf5*, *traf2*, *pak7*, and *mcl1* mRNA expression levels of WT, *jnk1*$^{-/-}$, *jnk2*$^{-/-}$, and *jnk3*$^{-/-}$ mice 12 h after KA treatment. Each value represents the mean ± SEM (n = 6/group). The *red baseline* indicates the basal expression level in untreated mice for each gene. $^{**}P < 0.01$ and $^{***}P < 0.001$ vs basal control WT; $^{\#}P < 0.05$, $^{\#\#}P < 0.01$, $^{\#\#\#}P < 0.001$ vs WT KA 12 h

the differential response between both KO (*jnk1*$^{-/-}$ and *jnk3*$^{-/-}$) and the absence of neuroprotection in *jnk2*$^{-/-}$ suggests that the response is not linked directly to the reduction of JNK pathway activity and therefore each isoform has a specific link with other cellular processes.

The inflammatory cascade after KA administration is mediated by an upregulation of pro- and anti-inflammatory cytokines that are secreted by astrocytes and microglia [48]. For that reason, in order to know more about the relationship between JNK1 and JNK3 isoforms and the induction of the neuroinflammation process, the expression of genes that encode cytokines such as *Il1β*, *Ifnγ*, *cox2*, *and ccl2* was evaluated 12 h after KA treatment. This time point was shown to be optimal to clearly identify differences in gene expression levels among the different genotypes. The differential increase in *cox2 and ccl2* mRNA levels reinforced an attenuation of the inflammation process in *jnk1*$^{-/-}$ and *jnk3*$^{-/-}$ mice. Along this line, Xu et al. [49] observed that *cox2* ablation results in decreased production of inflammatory cytokines after seizure induction. Despite the concurrence in the response of these cytokines in *jnk1*$^{-/-}$ and *jnk3*$^{-/-}$, other cytokines, such as *il1β and ifnγ*, were only attenuated in *jnk3*$^{-/-}$ mice, not in *jnk1*$^{-/-}$ mice. Taking into account the results obtained via immunofluorescence, which revealed that in *jnk1*$^{-/-}$ mice, the microglial immunoreactivity was not attenuated as in *jnk3*$^{-/-}$ mice, the secretion of *il1β* and *ifnγ* cytokines could be microglia specific. Therefore, although *jnk1*$^{-/-}$ and *jnk3*$^{-/-}$ showed neuroprotection against KA, the secretion of pro-

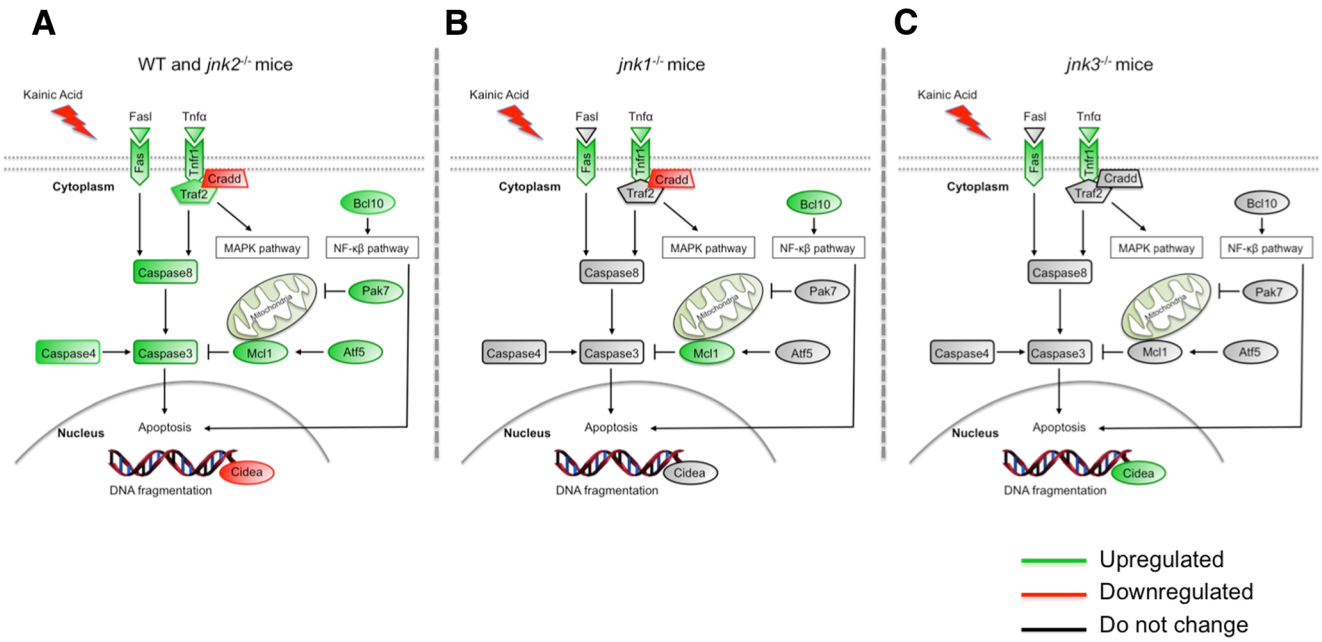

Fig. 9 Schematic representation of the effect of kainic acid treatment in the expression of apoptotic genes in WT and **a** *jnk2*$^{-/-}$, **b** *jnk1*$^{-/-}$, and **c** *jnk3*$^{-/-}$ mice. *Green boxes* indicate upregulation while *red boxes* correspond to downregulation of the genes with respect to WT KA. Unchanged expression is shown in *black*

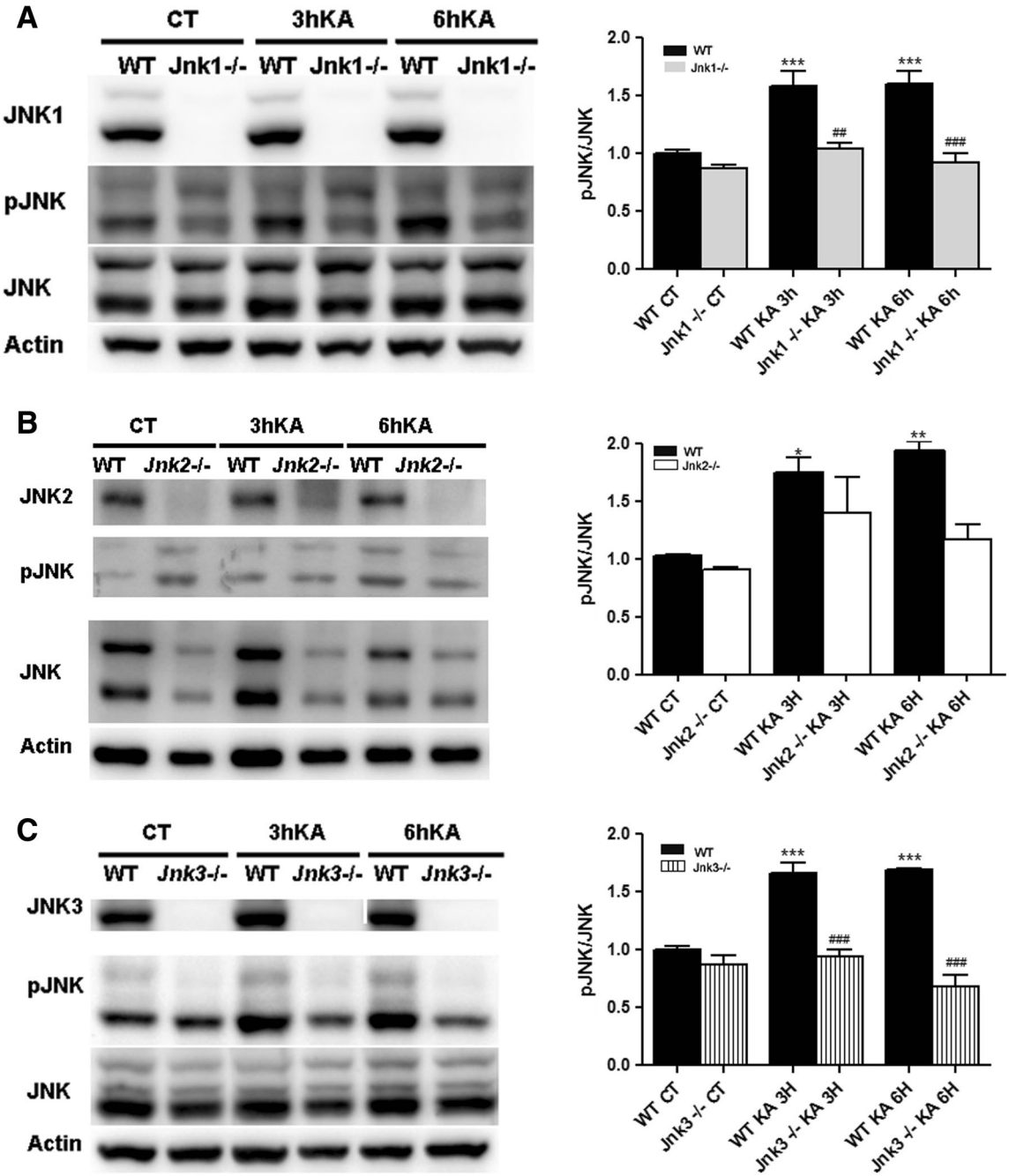

Fig. 10 p-JNK and total JNK protein levels of JNK KO and WT treated mice. Representative image of western blot against p-JNK and total JNK obtained from the hippocampus of brains after 3 and 6 h of KA treatment. **a** Pattern of pJNK and total JNK levels in *jnk1*$^{-/-}$ treated mice vs WT. *Graph bars* represent the mean ± SEM (n = 6/group). Statistical differences between control and treated animals were considered significant; ***$P < 0.001$ vs control WT; $^{\#\#}P < 0.01$ and $^{\#\#\#}P < 0.001$ vs control *jnk1*$^{-/-}$. **b** Pattern of pJNK and total JNK levels in *jnk2*$^{-/-}$ treated mice vs WT. *Graph bars* represent the mean ± SEM (n = 6/group). Statistical differences between control and treated animals were considered significant; *$P < 0.05$; **$P < 0.01$ vs control WT. **c** Pattern of pJNK and total JNK levels in *jnk3*$^{-/-}$ treated mice vs WT. Statistical differences between control and treated animals were considered significant; ***$P < 0.001$ vs control WT; $^{\#\#\#}P < 0.001$ vs control *jnk3*$^{-/-}$. In all cases, actine was used as a loading control

inflammatory cytokines was higher in *jnk1*$^{-/-}$ mice than in *jnk3*$^{-/-}$ mice. Notwithstanding, in view of the results obtained, it would be necessary to evaluate the expression levels of more pro-inflammatory and anti-inflammatory genes because their combination may be critical in controlling the progress of epileptogenesis as was discussed by Cho and Hsieh [50].

The differential inflammatory responses observed between *jnk1*$^{-/-}$ and *jnk3*$^{-/-}$ mice support that the neuroprotective

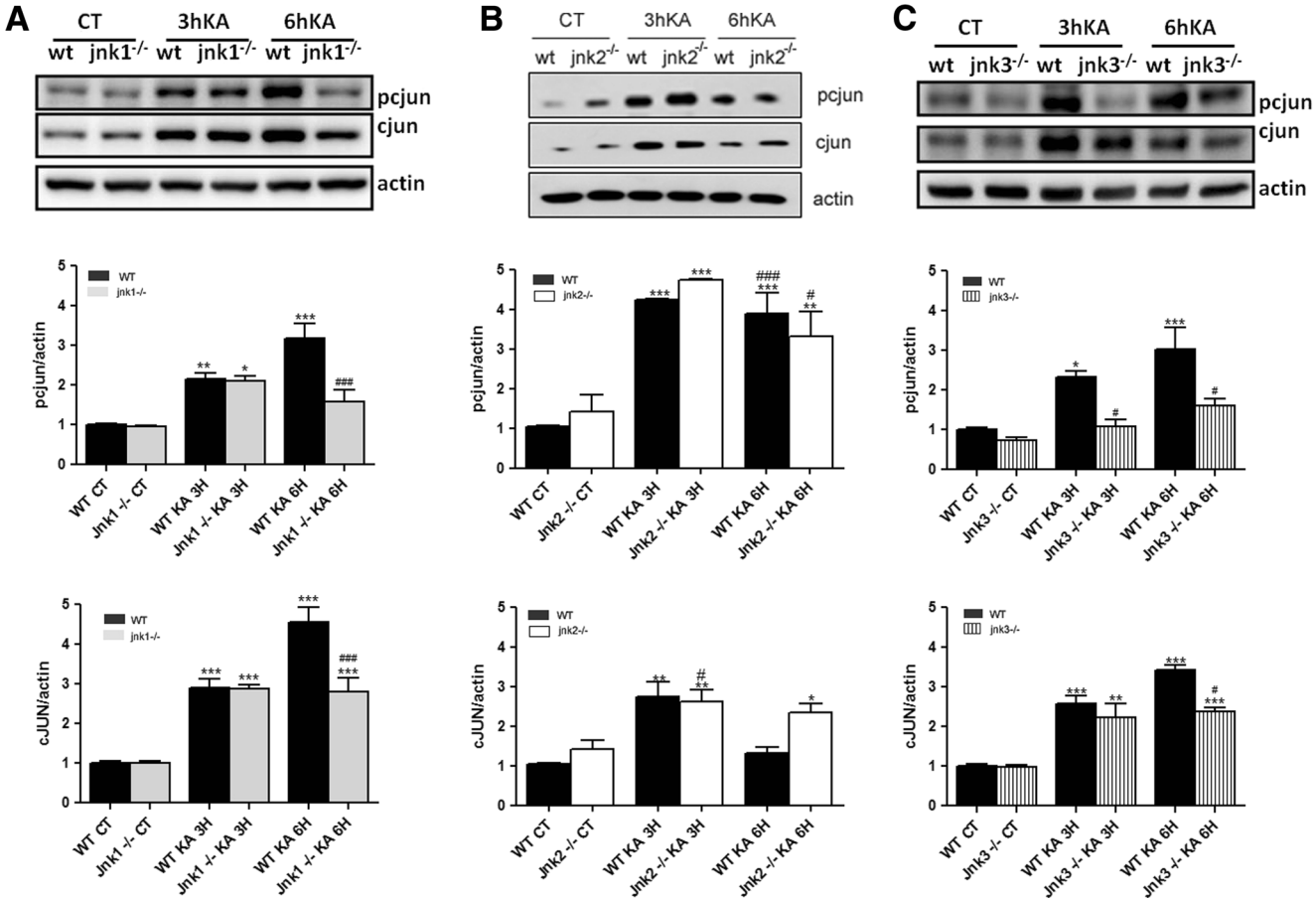

Fig. 11 p-c-Jun and total c-Jun protein levels of JNK KO and WT treated mice. Representative image of western blot against p-c-Jun and total c-Jun obtained from the hippocampus of brains after 3 and 6 h of KA treatment. **a** Pattern of p-c-Jun and total c-Jun levels in $jnk1^{-/-}$ treated mice vs WT. *Graph bars* represent the mean ± SEM (n = 6/group). Statistical differences between control and treated animals were considered significant; $^{*}P < 0.05$; $^{**}P < 0.01$, $^{***}P < 0.001$ vs control WT; $^{\#\#\#}P < 0.001$ vs control $jnk1^{-/-}$. **b** Pattern of p-c-Jun and total c-Jun levels in $jnk2^{-/-}$ treated mice vs WT. *Graph bars* represent the mean ± SEM (n = 6/group). Statistical differences between control and treated animals were considered significant; $^{**}P < 0.01$, $^{***}P < 0.001$ vs control WT; $^{\#}P < 0.05$, $^{\#\#\#}P < 0.001$ vs control $jnk2^{-/-}$. **c** Pattern of p-c-Jun and total c-Jun levels in $jnk3^{-/-}$ treated mice vs WT. *Graph bars* represent the mean ± SEM (n = 6/group). Statistical differences between control and treated animals were considered significant; $^{*}P < 0.05$; $^{**}P < 0.01$, $^{***}P < 0.001$ vs control WT; $^{\#}P < 0.05$ vs control $jnk3^{-/-}$. In all cases, actine was used as a loading control

effect of these isoforms does not occur through identical mechanisms.

The JNK3 and JNK1 Isoforms Control the Apoptotic Mechanisms That Are Induced in the KA Model

The Fasl/Fas pathway was downregulated in $jnk1^{-/-}$ and $jnk3^{-/-}$ mice compared to that in WT and in $jnk2^{-/-}$ mice after KA treatment, which suggests the existence of an intrinsic neuroprotection. This finding could explain why the upregulation of anti-apoptotic genes, such as *atf5*, *traf2*, and *pak7*, which occurred in WT and $jnk2^{-/-}$ mice was not required *in* $jnk1^{-/-}$ and $jnk3^{-/-}$ treated mice.

Specificity in gene control of each JNK isoform was observed following KA treatment. In this way, with the absence of JNK3, the expression levels of *bcl-10* and *cradd* after treatment were maintained, unlike what occurred in the other genotypes. Otherwise, *cidea* expression is controlled by the JNK1 isoform because the levels of *cidea* remained unchanged or repressed in $jnk1^{-/-}$ mice, unlike what happened in the other KO mice. These results suggest that the neuroprotection observed with the lack of JNK1 after KA treatment may be dependent on the absence of DNA fragmentation. This differential gene control between the JNK1 and JNK3 isoforms is supported by the previous results of our group in which a distinct pathway activation was observed between $jnk1^{-/-}$ and $jnk3^{-/-}$ mice [51].

Conclusion

In spite of some studies that have shown that the inhibition of JNK might play a role in the prevention of neurodegenerative diseases and inflammatory processes (Wang et al. 2014;

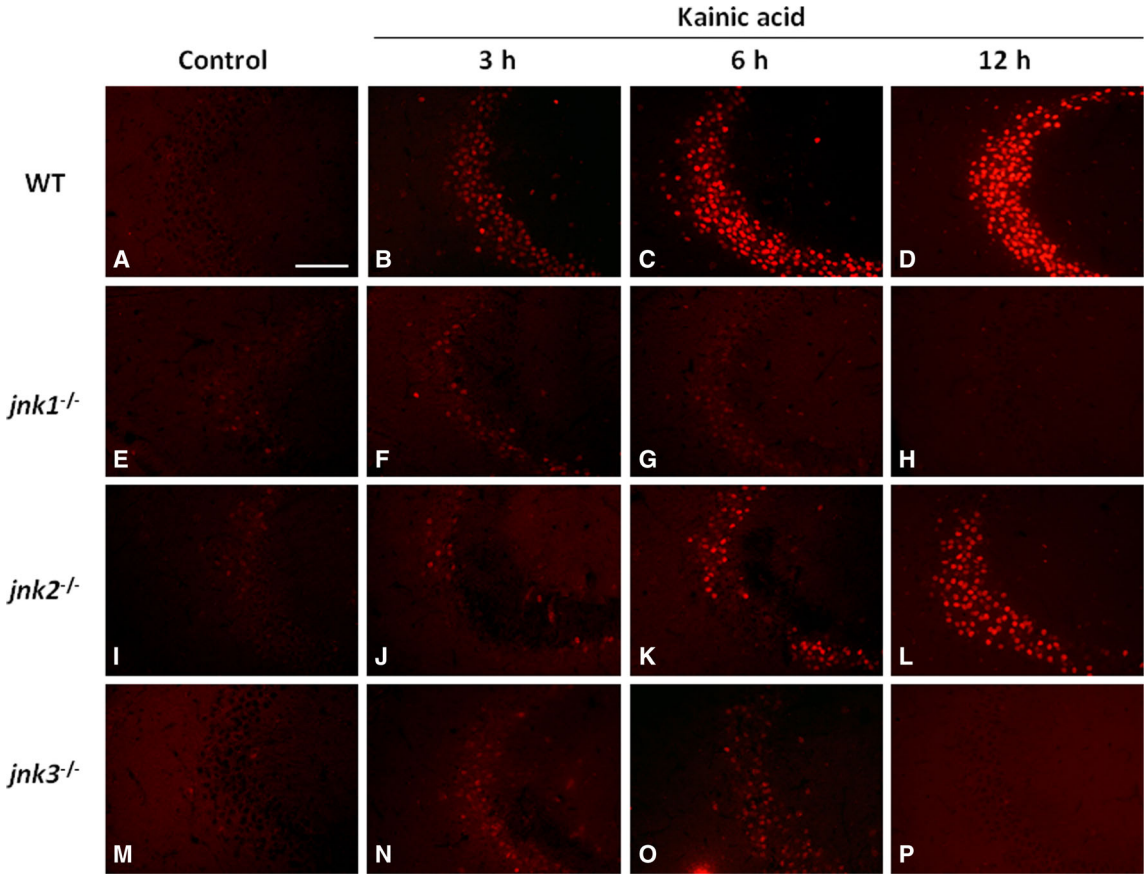

Fig. 12 Immunofluorescence against p-c-Jun in the brains of JNK KO and WT treated with KA. Cell distribution pattern of p-c-Jun immunopositive cells in the CA3 hippocampal area, at 3, 6, and 12 h after KA treatment. **a**–**d** WT, **e**–**h** *jnk1*$^{-/-}$, **i**–**l** *jnk2*$^{-/-}$, and **m**–**p** *jnk3*$^{-/-}$ mice. *Scale bar* 100 μm

Taylor et al. 2013), the JNK inhibitory drugs that have been identified thus far are quite non-specific, resulting in cross-talk among different targets and triggering important side effects. Our data support that JNK1 and JNK3 participate in modulating neurodegeneration and neuroinflammation processes following different cell mechanisms, after KA-induced excitotoxicity, directly related to seizure appearance. Therefore, the JNK3 and JNK1 isoforms may be potential specific therapeutic targets for the reduction of neurodegeneration and brain inflammatory responses in convulsive status epilepticus and neurodegenerative diseases.

AD, Alzheimer's disease; AMPA, α-amino-3-hydroxy-5-methyl-4-isoxazolepropionic acid; Atf5, activating transcription factor 5; Bcl10, B cell CLL/lymphoma 10; Casp, cysteine-aspartic proteases; Ccl2, chemokine (C-C motif) ligand 2; c-Fos, proto-oncogene; Cidea, cell death-inducing DFFA-like effector a; c-Jun, Jun proto-oncogene, AP-1 transcription factor subunit; Cox2, cyclooxygenase 2 gene; GFAP, glial fibrillary acidic protein; iba-1, ionized calcium binding adaptor molecule 1; Ifnγ, interferon gamma gene; Il1β, interleukin-1 alpha gene; IRS, insulin receptor substrates; i.p., intraperitoneal injection; JNKs, c-Jun N-terminal kinases; JNK1, JNK2, and JNK3, JNK isoforms; jnk1−/− knockout mice for JNK1; jnk2−/− knockout mice for JNK2; jnk3−/− knockout mice for JNK3; KA, kainic acid; KO, JNK knockout mice; Fas, Fas cell surface death receptor; Fasl, Fas ligand; FJ, Fluoro-Jade B; MAP kinases, mitogen-activated-protein-kinase; MAP2, microtubule-associated protein 2; Mcl1, monocyte chemoattractant protein-1 gene; MPTP, 1-methyl-4-phenyl-1,2,4,6-tetrahydropyridine; O/N, overnight; Pak7, serine/threonine-protein kinase; PB, phosphate buffer WT, wild-type; PBS, phosphate-buffered saline; p-c-Jun, phospho-c-Jun; PD, Parkinson's disease; p-JNK, phospho-JNK; RT, room temperature; SDA-PAGE, sodium dodecyl sulfate polyacrylamide gel electrophoresis; SDS, sodium dodecyl sulfate; SEM, standard error of mean; SMTNL2, smoothelin-like 2; Tnfα1, tumor necrosis factor; Tnfr1, tumor necrosis factor receptor; Traf2, TNF receptor-associated factor 2

Acknowledgements We thank Richard A. Flavell, Ph.D, a Howard Hughes Medical Institute ("HHMI") Investigator at Yale University School of Medicine, Department of Immunobiology, for providing knockout mice.

This research was supported by the following:

• Ministerio Español de Ciéncia y Innovación (PI2016/01)

• Centro de Investigación Biomédica en Red de Enfermedades Neurodegenerativas (CIBERNED) CB06/05/0024

• Consejo Nacional de Ciencia y Tecnología (CONACYT). Project No. 177594 (CBZ)
• Postdoctoral Fellowship CONACYT. No. 298337 and Doctoral Program in Sciences in Molecular Biology in Medicine, LGAC Molecular Bases of Chronic Diseases-Degenerative and its Applications (000091, PNPC, CONACYT)
• Research team from UB and URV belongs to 2014SGR-525 from Generalitat de Catalunya

Authors' Contributions CA and EV designed the experiments. CA wrote the manuscript. LL, FJ, and EV performed the kainic acid treatment and sample preparation. LL and FJ performed RNA extraction, quantitative real-time PCR, and western blots. FJ and JO performed Fluoro-Jade staining. LL, FJ, RD, and EV performed immunochemistry and immunofluorescence experiments. JF, AC, and CB assisted with the development of experimental procedures, data processing, and statistical analyses. All authors read and approved the final manuscript.

Compliance with Ethical Standards

Conflict of Interest The authors declare that they have no conflict of interest.

References

1. Davis RJ (1999) Signal transduction by the c-Jun N-terminal kinase. Biochem Soc Symp 64:1–12
2. Zdrojewska J, Coffey ET (2014) The impact of JNK on neuronal migration. Adv Exp Med Biol 800:37–57. doi:10.1007/978-94-007-7687-6_3
3. Ventura J-J, Hübner A, Zhang C et al (2006) Chemical genetic analysis of the time course of signal transduction by JNK. Mol Cell 21:701–710. doi:10.1016/j.molcel.2006.01.018
4. Gupta S, Barrett T, Whitmarsh AJ et al (1996) Selective interaction of JNK protein kinase isoforms with transcription factors. EMBO J 15:2760–2770
5. Karin M (1995) The regulation of AP-1 activity by mitogen-activated protein kinases. J Biol Chem 270:16483–16486. doi:10.1098/rstb.1996.0008
6. Chang L, Jones Y, Ellisman MH et al (2003) JNK1 is required for maintenance of neuronal microtubules and controls phosphorylation of microtubule-associated proteins. Dev Cell 4:521–533. doi:10.1016/S1534-5807(03)00094-7
7. Tararuk T, Östman N, Li W et al (2006) JNK1 phosphorylation of SCG10 determines microtubule dynamics and axodendritic length. J Cell Biol 173:265–277. doi:10.1083/jcb.200511055
8. Tanti J-F, Jager J (2009) Cellular mechanisms of insulin resistance: role of stress-regulated serine kinases and insulin receptor substrates (IRS) serine phosphorylation. Curr Opin Pharmacol 9:753–762. doi:10.1016/j.coph.2009.07.004
9. Gordon EA, Whisenant TC, Zeller M et al (2013) Combining docking site and phosphosite predictions to find new substrates: identification of smoothelin-like-2 (SMTNL2) as a c-Jun N-terminal kinase (JNK) substrate. Cell Signal 25:2518–2529. doi:10.1016/j.cellsig.2013.08.004
10. Kwak D, Choi S, Jeong H et al (2012) Osmotic stress regulates mammalian target of rapamycin (mTOR) complex 1 via c-Jun N-terminal kinase (JNK)-mediated raptor protein phosphorylation. J Biol Chem 287:18398–18407. doi:10.1074/jbc.M111.326538
11. Dong C, Yang DD, Wysk M et al (1998) Defective T cell differentiation in the absence of Jnk1. Science (New York, NY) 282:2092–2095. doi:10.1126/science.282.5396.2092
12. Yang DD, Conze D, Whitmarsh AJ et al (1998) Differentiation of CD4+ T cells to Th1 cells requires MAP kinase JNK2. Immunity 9:575–585 **doi: S1074-7613(00)80640-8 [pii]**
13. Yang DD, Kuan CY, Whitmarsh AJ et al (1997) Absence of excitotoxicity-induced apoptosis in the hippocampus of mice lacking the Jnk3 gene. Nature 389:865–870. doi:10.1038/39899
14. Li QM, Tep C, Yune TY et al (2007a) Opposite regulation of oligodendrocyte apoptosis by JNK3 and Pin1 after spinal cord injury. J Neurosci 27:8395–8404. doi:10.1523/JNEUROSCI.2478-07.2007
15. Li T, Quan Lan J, Fredholm BB et al (2007b) Adenosine dysfunction in astrogliosis: cause for seizure generation? Neuron Glia Biol 3:353–366. doi:10.1017/S1740925X0800015X
16. De Lemos L, Junyent F, Verdaguer E et al (2010) Differences in activation of ERK1/2 and p38 kinase in Jnk3 null mice following KA treatment. J Neurochem 114:1315–1322. doi:10.1111/j.1471-4159.2010.06853.x
17. Hunot S, Vila M, Teismann P et al (2004) JNK-mediated induction of cyclooxygenase 2 is required for neurodegeneration in a mouse model of Parkinson's disease. Proc Natl Acad Sci U S A 101:665–670. doi:10.1073/pnas.0307453101
18. Yoon SO, Park DJ, Ryu JC et al (2012) JNK3 perpetuates metabolic stress induced by Aβ peptides. Neuron 75:824–837. doi:10.1016/j.neuron.2012.06.024
19. Sabapathy K, Jochum W, Hochedlinger K et al (1999) Defective neural tube morphogenesis and altered apoptosis in the absence of both JNK1 and JNK2. Mech Dev 89:115–124. doi:10.1016/S0925-4773(99)00213-0
20. Kuan CY, Yang DD, Samanta Roy DR et al (1999) The Jnk1 and Jnk2 protein kinases are required for regional specific apoptosis during early brain development. Neuron 22:667–676
21. Ben-Ari Y, Lagowska J (1978) Epileptogenic action of intra-amygdaloid injection of kainic acid. Comptes rendus hebdomadaires des seances de l'Academie des sciences Serie D: Sciences naturelles 287:813–816
22. Ben-Ari Y, Tremblay E, Ottersen OP (1979) Primary and secondary cerebral lesions produced by kainic acid injections in the rat. Comptes rendus des seances de l'Academie des sciences Serie D, Sciences naturelles 288:991–994
23. Ben-Ari Y (1985) Limbic seizure and brain damage produced by kainic acid: mechanisms and relevance to human temporal lobe epilepsy. Neuroscience 14:375–403. doi:10.1016/0306-4522(85)90299-4
24. Ben-Ari Y, Cossart R (2000) Kainate, a double agent that generates seizures: two decades of progress. Trends Neurosci 23:580–587. doi:10.1016/S0166-2236(00)01659-3
25. Benkovic SA, O'Callaghan JP, Miller DB (2004) Sensitive indicators of injury reveal hippocampal damage in C57BL/6J mice treated with kainic acid in the absence of tonic-clonic seizures. Brain Res 1024:59–76. doi:10.1016/j.brainres.2004.07.021
26. Auladell C, de Lemos L, Verdaguer E et al (2017a) Role of JNK isoforms in the kainic acid experimental model of epilepsy and neurodegeneration. Front biosci (Landmark edition) 22:795–814
27. Jeon SH, Kim YS, Bae C-D, Park J-B (2000) Activation of JNK and p38 in rat hippocampus after kainic acid induced seizure. Exp Mol Med 32:227–230
28. Spigolon G, Veronesi C, Bonny C, Vercelli A (2010) c-Jun N-terminal kinase signaling pathway in excitotoxic cell death following kainic acid-induced status epilepticus. Eur J Neurosci 31:1261–1272. doi:10.1111/j.1460-9568.2010.07158.x
29. Zhao Y, Spigolon G, Bonny C et al (2012) The JNK inhibitor D-JNKI-1 blocks apoptotic JNK signaling in brain mitochondria. Mol Cell Neurosci 49:300–310. doi:10.1016/j.mcn.2011.12.005
30. Bozzi Y, Vallone D, Borrelli E (2000) Neuroprotective role of dopamine against hippocampal cell death. J Neurosci 20

31. Junyent F, Utrera J, Romero R et al (2009) Prevention of epilepsy by taurine treatments in mice experimental model. J Neurosci Res 87:1500–1508. doi:10.1002/jnr.21950
32. Tripathi PP, Santorufo G, Brilli E et al (2010) Kainic acid-induced seizures activate GSK-3β in the hippocampus of D2R−/− mice. Neuroreport 21:846–850. doi:10.1097/WNR.0b013e32833d5891
33. Rossi AR, Angelo MF, Villarreal A et al (2013) Gabapentin administration reduces reactive gliosis and neurodegeneration after pilocarpine-induced status epilepticus. PLoS One 8:e78516. doi:10.1371/journal.pone.0078516
34. George Paxinos KF (2012) Paxinos and Franklin's the mouse brain in stereotaxic coordinates. academic press, São Paulo, p. 360
35. Schmued LC, Hopkins KJ (2000) Fluoro-Jade B: a high affinity fluorescent marker for the localization of neuronal degeneration. Brain Res 874:123–130. doi:10.1016/S0006-8993(00)02513-0
36. Chen Z, Duan R-S, Quezada HC et al (2005) Increased microglial activation and astrogliosis after intranasal administration of kainic acid in C57BL/6 mice. J Neurobiol 62:207–218. doi:10.1002/neu.20099
37. Ettcheto M, Junyent F, de Lemos L et al (2015a) Mice lacking functional Fas death receptors are protected from kainic acid-induced apoptosis in the hippocampus. Mol Neurobiol 52:120–129. doi:10.1007/s12035-014-8836-0
38. Gall C, Lauterborn J, Isackson P, White J (1990) Seizures, neuropeptide regulation, and mRNA expression in the hippocampus. Prog Brain Res 83:371–390
39. Pan J, Xiao Q, Sheng CY et al (2009) Blockade of the translocation and activation of c-Jun N-terminal kinase 3 (JNK3) attenuates dopaminergic neuronal damage in mouse model of Parkinson's disease. Neurochem Int 54:418–425. doi:10.1016/j.neuint.2009.01.013
40. Condorelli DF, Trovato-Salinaro A, Mudò G et al (2003) Cellular expression of connexins in the rat brain: neuronal localization, effects of kainate-induced seizures and expression in apoptotic neuronal cells. Eur J Neurosci 18:1807–1827. doi:10.1046/j.1460-9568.2003.02910.x
41. Cui J, Zhang M, Zhang Y, Xu Z (2007) JNK pathway: diseases and therapeutic potential. Acta Pharmacol Sin 28:601–608. doi:10.1111/j.1745-7254.2007.00579.x
42. Park B (2014) JNK1-mediated phosphorylation of Smac/DIABLO at the serine 6 residue is functionally linked to its mitochondrial release during TNF-α-induced apoptosis of HeLa cells. Mol Med Rep. doi:10.3892/mmr.2014.2625
43. Mohammad H, Marchisella F, Ortega-Martinez S et al (2016) JNK1 controls adult hippocampal neurogenesis and imposes cell-autonomous control of anxiety behaviour from the neurogenic niche. Mol Psychiatry. doi:10.1038/mp.2016.203
44. Komulainen E, Zdrojewska J, Freemantle E et al (2014) JNK1 controls dendritic field size in L2/3 and L5 of the motor cortex, constrains soma size, and influences fine motor coordination. Front Cell Neurosci 8:272. doi:10.3389/fncel.2014.00272
45. Barnat M, Enslen H, Propst F et al (2010) Distinct roles of c-Jun N-terminal kinase isoforms in neurite initiation and elongation during axonal regeneration. J Neurosci 30:7804–7816. doi:10.1523/JNEUROSCI.0372-10.2010
46. Ekmark-Lewén S, Flygt J, Kiwanuka O et al (2013) Traumatic axonal injury in the mouse is accompanied by a dynamic inflammatory response, astroglial reactivity and complex behavioral changes. J Neuroinflammation 10:44. doi:10.1186/1742-2094-10-44
47. Devinsky O, Vezzani A, Najjar S et al (2013) Glia and epilepsy: excitability and inflammation. Trends Neurosci 36:174–184. doi:10.1016/j.tins.2012.11.008
48. Ziebell JM, Morganti-Kossmann MC (2010) Involvement of pro- and anti-inflammatory cytokines and chemokines in the pathophysiology of traumatic brain injury. Neurotherapeutics 7:22–30. doi:10.1016/j.nurt.2009.10.016
49. Xu D, Miller SD, Koh S (2013) Immune mechanisms in epileptogenesis. Front Cell Neurosci. doi:10.3389/fncel.2013.00195
50. Cho KO, Hsieh J (2016) Microglial TLR9: guardians of homeostatic hippocampal neurogenesis. Epilepsy Curr 16:39–40. doi:10.5698/1535-7597-16.1.39
51. Junyent F, De Lemos L, Verdaguer E et al (2011) Gene expression profile in JNK3 null mice: a novel specific activation of the PI3K/AKT pathway. J Neurochem 117:244–252. doi:10.1111/j.1471-4159.2011.07195.x